Distinct patterns of spatial attentional modulation of steady state visual evoked magnetic fields (SSVEFs) in subdivisions of the human early visual cortex

Stephan Moratti[1], Christopher Gundlach[2], Javi Echegaray[2], and Matthias Müller[2]

[1]Universidad Complutense de Madrid
[2]Universität Leipzig

June 12, 2023

Abstract

In recent years, steady state visual evoked potentials (SSVEPs) became an increasingly valuable tool to investigate neural dynamics of competitive attentional interactions and brain computer interfaces. This is due to their good signal-to-noise ratio, allowing for single trial analysis and their ongoing oscillating nature that enables to analyze temporal dynamics of facilitation and suppression. Given the popularity of SSVEPs, it is surprising that only a few studies looked at the cortical sources of these responses. This is in particular the case when searching for studies that assessed the cortical sources of attentional SSVEP amplitude modulations. To address this issue, we used a typical spatial attention task and recorded neuromagnetic fields (MEG) while presenting frequency-tagged stimuli in the left and right visual field, respectively. Importantly, we controlled for attentional deployment in a baseline period before the shifting cue. Subjects either attended to a central fixation cross or to two peripheral stimuli simultaneously. Results clearly showed that signal sources and attention effects were restricted to early visual cortex: V1, V2, hMT+, precuneus, occipital-parietal and inferior-temporal cortex. When subjects attended to central fixation first, shifting attention to one of the peripheral stimuli resulted in a significant activation increase for the to-be-attended stimulus with no activation decrease for the to-be-ignored stimulus in hMT+ and inferio-temporal cortex, but significant SSVEF decreases from V1 to occipito-parietal cortex. When attention was first deployed to both rings, shifting attention away from one ring basically resulted in a significant activation decrease in all areas for the then to-be-ignored stimulus.

Distinct patterns of spatial attentional modulation of steady state visual evoked magnetic fields (SSVEFs) in subdivisions of the human early visual cortex

* Stephan Moratti[1,2], Christopher Gundlach[3], Javier de Echegaray[3], Matthias M. Müller[3]

[1]Department of Experimental Psychology, Complutense University of Madrid, Spain

[2]Center for Cognitive and Computational Neuroscience, Complutense University of Madrid, Spain

[3]Wilhelm Wundt Institute for Psychology, University of Leipzig, Germany

***Corresponding Author:**

Stephan Moratti, PhD

Department of Experimental Psychology Faculty of Psychology

Complutense University of Madrid, Spain

Email: smoratti@ucm.es

Acknowledgements: Research was supported by a grant from the German Research Foundation (MU 972/24-1). JM was supported by a grant from the Complutense University of Madrid and Santander bank.

The authors declare to have no conflict of interest. Data is available upon request to the first author SM

Abstract

In recent years, steady state visual evoked potentials (SSVEPs) became an increasingly valuable tool to investigate neural dynamics of competitive attentional interactions and brain computer interfaces. This is due to their good signal-to-noise ratio, allowing for single trial analysis and their ongoing oscillating nature that enables to analyze temporal dynamics of facilitation and suppression. Given the popularity of SSVEPs, it is surprising that only a few studies looked at the cortical sources of these responses. This is in particular the case when searching for studies that assessed the cortical sources of attentional SSVEP amplitude modulations. To address this issue, we used a typical spatial attention task and recorded neuromagnetic fields (MEG) while presenting frequency-tagged stimuli in the left and right visual field, respectively. Importantly, we controlled for attentional deployment in a baseline period before the shifting cue. Subjects either attended to a central fixation cross or to two peripheral stimuli simultaneously. Results clearly showed that signal sources and attention effects were restricted to early visual cortex: V1, V2, hMT+, precuneus, occipital-parietal and inferior-temporal cortex. When subjects attended to central fixation first, shifting attention to one of the peripheral stimuli resulted in a significant activation increase for the to-be-attended stimulus with no activation decrease for the to-be-ignored stimulus in hMT+ and inferio-temporal cortex, but significant SSVEF decreases from V1 to occipito-parietal cortex. When attention was first deployed to both rings, shifting attention away from one ring basically resulted in a significant activation decrease in all areas for the then to-be-ignored stimulus.

Impact statement

Although the cortical generators of steady state visual evoked responses as recorded by EEG or MEG (SSVEPs or SSVEFs, respectively) have been described in humans, how these generators are involved in the modulation of these evoked oscillatory responses by spatial attention is less known. Here, we describe how distinct sub-divisions of the early human visual cortex contribute differently to the modulation of SSVEFs by spatial attention.

Introduction

Steady state visual evoked potentials (SSVEPs) and their magnetic counterpart (SSVEFs) experienced a remarkable evolution in the cognitive neurosciences and brain computer interface literature. The number of publications using or investigating SSVEPs increased significantly during the last 30 years. For example, a snapshot of the last three years, i.e., from 2020 to 2022, Web of Science lists 298 publications with the words "SSVEP" or "steady state visual evoked" in the title. Ten years ago, i.e., between 2010 and 2012 the list contains 81 publications, and this went down to 14 between 2000 and 2003 and to 16 publications between 1990 and 1992, respectively.

This evolution is not too surprising, given the advantage that SSVEPs provide to investigate competitive attentional selection mechanisms in the visual (see for summaries Müller 2014, Norcia et al. 2015), auditory (cf. Linden et al. 1987, Woldorff and Hillyard 1991, Makeig et al. 1996, Picton et al. 2003) and somatosensory domain (Snyder 1992, Tobimatsu et al. 1999, Giabbiconi et al. 2007, Adler et al. 2009, Goltz et al. 2015, Pang and Müller 2015) and as a robust signal for brain computer interfaces (for a review see Zhu et al. 2010). The biggest advantage of SSVEPs is their high signal-to-noise ratio, in particular for frequencies in the range of 8-15 Hz, that allows to extract them even in single trials. Their ongoing oscillatory nature permits to track exact time courses of competitive interactions or attentional resource allocation in multi element stimulus designs, in particular in the visual domain (cf. Müller et al. 1998, Antonov et al. 2020, Gundlach et al. 2020, Gundlach et al. 2022). The power of frequency-tagged stimuli as a valuable tool in scientific and applied

settings was nicely reviewed in a 2015 paper by Norcia and colleagues (Norcia et al. 2015), and we would like to refer interested readers to that paper, rather than listing all the areas here.

In visual attention research, it was demonstrated that the amplitude of SSVEPs increased significantly when a flickering stimulus was attended, compared to when it was ignored. This modulation pattern has been observed for spatial (cf. Morgan et al. 1996, Müller et al. 1998, Müller and Hübner 2002, Müller et al. 2003, Walter et al. 2014), feature-based (cf. Müller et al. 2006, Andersen et al. 2008, Andersen et al. 2013, Störmer and Alvarez 2014, Andersen et al. 2015) and object-based attention (cf. Brummerloh et al. 2019, Brummerloh and Müller 2019, Adamian et al. 2020). Despite the wealth of studies using SSVEPs as a tool, surprisingly few studies were interested in the underlying cortical generators. Among the earliest studies was a study by Müller and colleagues (Müller et al. 1997), using a 37-channels magnetometer and a single equivalent current dipole model for steady state responses at 6, 12 and 15 Hz. Results revealed sources in early visual cortex, and suggested differential activation patterns as a function of stimulation frequency. One year later, Hillyard and colleagues (Hillyard et al. 1997), in a combined electroencephalographic (EEG) and functional magnetic resonance imaging (fMRI) study, reported sources in ventral and lateral extrastriate visual areas in a visual spatial attention task, that were basically replicated in another spatial attention task study implementing a pure EEG-based source analysis of SSVEP signals (Müller et al. 1998). While these early studies found sources of SSVEPs predominately in extrastriate cortex, studies that were conducted after the turn of the millennium consistently found generators of the SSVEP in V1 as well. Pastor and colleagues (Pastor et al. 2003) presented their subjects a broad range of flickering stimuli from 2-90 Hz while they recorded EEG and used some of these frequencies during positron emission tomography (PET) recordings. They reported significant activation in primary visual cortex (see also Pastor et al. 2007). These results are in line with an MEG study from Fawcett and colleagues (Fawcett et al. 2004) who also presented their subjects a broad range of frequencies up to 21 Hz, and by Kaufmann and colleagues (Kaufmann et al. 2001) for the same frequency range in an fMRI study. The most extensive study, however, was presented by DiRusso and colleagues (Di Russo et al. 2007). In their study a 6 Hz Gabor stimulus was presented in a passive viewing task. They recorded EEG and fMRI, and used retinotopic mapping to estimate SSVEP sources in visual cortex. They found SSVEP generators in V1, V3A, V4/V8 and hMT+/V5.

In summary, these studies provided clear evidence, that the generators of SSVEPs are located in early visual cortex that are linked to low-level visual processing. This holds for a broad range of flicker frequencies and stimulus types (for flickering facial stimuli see Wieser and Keil 2011). However, when it comes to the question of what are the sources that generate attention effects, *e. g. the attentional*SSVEP amplitude enhancement, these studies have only limited value. First, almost all studies used a passive viewing task, and therefore were agnostic to attentional modulations. Second, in the fMRI study by Hillyard et al. (1997) conditions in which attention was deployed to one side of the screen were contrasted with passive viewing. This did not allow to control for attentional deployment during passive viewing (*e. g.* did subjects attend to the fixation cross, or to both flickering stimuli, or attended to both flickers in an arbitrary alternating manner during 36 seconds of recording in blocks of passive viewing?). In order to get a better estimate of cortical sources that contribute to attention effects, it is mandatory to control for subjects' attentional state/deployment during a reference or baseline stimulation period.

In the current MEG study, we used a spatial attention design with a flickering stimulus presented in the left and right visual hemifield, respectively. In a trial-by-trial fashion, in an interval between 1500 and 2000 ms after flicker onset, subjects were cued to shift attention to the left or right stimulus and to perform a task at the attended location/stimulus. In order to control for attentional deployment during the pre-cue period (i.e. baseline), subjects either attended to the fixation cross or to both stimuli in the left and right visual hemifields and performed a detection task associated with the respective spatial location(s). With this manipulation we were able to (a) estimate the cortical generators while attention was focused away from the peripheral stimuli (i.e. attend fixation cross), (b) when they attended to both stimuli (left and right), and (c) the contribution of cortical areas of attentional amplitude enhancement in the post-cue period, relative to the two pre-cue baseline conditions,.

Methods

Participants

Twenty healthy participants (13 females, one left-handed, mean age 20.5 years, range: 18 years to 27 years) volunteered in the study. The sample size was determined based on a previous EEG study of ours (Gundlach et al. 2020) as we used an almost identical paradigm. All participants had normal or corrected to normal vision and no history of photic epilepsy. The study had full ethical approval from the local ethics committee according to the Declaration of Helsinki and all participants gave written informed consent. We confirm that all methods were performed in accordance with the relevant guidelines and regulations following the Spanish and European law (Ley Orgánica 15/ 1999 de Protección de datos de Carácter Personal LOPD y Real Decreto 994/ 1999).

Stimuli

The same stimuli as in Gundlach et al. (2020) were used. All stimuli were created using the Psychtoolbox 3 (Kleiner et al. 2007) running on a PC with a Windows 8 operating system (Microsoft Cooperation). All visual stimuli were presented in a magnetically shielded room by a video projector (Panasonic PT-D7700E, 60 Hz refresh rate) via a mirror system. The distance between the projection screen (45 cm by 33.5 cm) and the participants was kept constant at 133.5 cm. The stimuli display consisted of two rings presented at 6.4^{o} to the left and right of central fixation cross (0.25^{o} by 0.25^{o}). The outer and inner diameter of the two rings were 4.6^{o} and 1.8^{o}, respectively. The background color of the screen was set to 30% of maximum white color (luminance 13 cd/ m^2). In order to evoke steady state visual evoked fields (SSVEFs) both rings flickered at 12 Hz and 15 Hz each, whereby the assignment of each flicker frequency to the left or right visual field was counter-balanced across subjects. The rings had a luminance of 70% of maximum white color (60 cd/ m^2) during the on-frames. For one half of the participants, the fixation cross target stimuli consisted of small decreases of the either vertical or horizontal length by 0.05^{o} in visual angle depicted for 60 ms. Increases of the same size served as distractor events. For the other half of participants, the target and distractor stimuli were reversed.

For the pre-cue task, target events for the peripheral rings were luminance decreases of a small segment of both rings (10^{o}) ranging between 55 % to 65 % of maximum white screen color (8 cd/ m^2 to 23 cd/ m^2) lasting for 150 ms. The position of the luminance reduced segment was chosen randomly between 0^{o} and 360^{o} around an arc spanning each of the two rings. Changes of luminance of the segment in only one of the two rings were defined as distractors. For the post-cue task (see below), luminance changes of the peripheral ring in the visual hemifield that had to be attended, defined a target event, whereas changes in the opposite hemifield were considered as distractors.

Procedure and task

After subjects were familiarized with the MEG chamber, a written informed consent was given and signed. Then, subjects were seated in the shielded room placing their head under the MEG helmet. The experiment consisted of a speeded detection paradigm similar to the experiment published by Gundlach et al. (2020). In general, a spatial cueing design with a pre-cue baseline task was utilized. Before a spatial cue indicated which visual hemifield had to be attended, participants performed a detection task. Thereby, the volunteers had to focus onto the central fixation cross in order to detect small size changes of the cross or extend spatial attention to the peripheral rings to detect segments of luminance changes within the rings at both visual hemifields simultaneously. The central fixation and peripheral rings conditions were assigned to two blocks of 240 trials each. Half of the participants started with the central fixation condition and then were administered the task that required attending the peripheral rings. The other half of the volunteers executed the tasks in reverse order. Each block contained 60 target, 60 distractor and 120 trials without any changes (no events). Targets and distractors for both pre-cue tasks were presented randomly within a time interval between 300 ms after trial onset and 500 ms before the presentation of the post-cue task (see below).

The pre-cue task duration varied randomly between 1500 ms to 2000 ms. Then, the fixation cross changed its

color either to red or blue indicating that the left or right visual hemifield had to be attended, respectively. The assignment of the color and hemifield was counter-balanced across participants. During the post-cue time interval, ranging from 3000 ms to 3500 ms, participants had to detect luminance decreases of a small segment of one of the peripheral rings (as in the pre-cue task). However, targets were only luminance changes in the to-be-attended visual hemifield. Luminance changes in segments of the ring in the to-be-ignored visual hemifield were considered as distractors. During the post-cue interval one, two or no events could occur. The events (targets or distractors) were presented between 300 ms after the post-cue and 500 ms before the trial end but were separated by at least 800 ms if two events occurred. The participants had to indicate the detection of a target in pre- and post-cue trials with a button press of the right index finger (half of the participants had to use the left index finger). The combinations of pre-cue (attend fixation cross vs. attend peripheral rings) and post-cue tasks (attend left vs. right visual hemifield) were fully balanced and each condition was repeated 120 times resulting in 480 trials in total. The experiment started with 12 practice trials (6 pre-cue fixation and 6 pre-cue peripheral rings trials).

Behavioral Analysis

Responses (button presses) after a target were considered as hits. Button presses after a distractor, or no event were scored as false alarms. Responses with latencies greater than 1 s were discarded from analysis.

MEG data acquisition and pre-processing

MEG data was continuously recorded (600 Hz sample rate, 0.1 Hz to 200 Hz online-filter) using a 306-channel (102 magnetometers, 204 orthogonal gradiometers pairs) system (Elekta-Neuromag® VectorView, Helsinki, Finland, 2005). For the depiction of sensor space MEG data only gradiometers will be shown as their magnetic flux topographies are easier to interpret. However, all cortical source space analyses (see below) were done based on all gradio- and magnetometer sensors. For artifact monitoring the electrooculogram (EOG) was recorded with electrodes attached above, below, left to and right to the outer canthus. The electrocardiogram (ECG) was recorded with electrodes placed at the left mid clavicle and lower right rib bone. Additionally, one electrode was attached to the left earlobe serving as the ground electrode. EOG and ECG were recorded simultaneously using standard Au electrodes (NSC Electromedicina) with the same sample frequency and on-line filters as the MEG data.

MEG data were spatially filtered using the temporal signal space separation (tSSS) algorithm implemented in Neuromag® MEG software (Taulu and Hari 2009). Eye blinks and cardiac artefacts were removed from data by independent component analysis (ICA-JADE) implemented in the Brainstorm software (Tadel et al. 2011) (*https://neuroimage.usc.edu/brainstorm/*). Then for each pre-cue trial (attend central fixation cross and attend peripheral rings) and participants epochs from -1 s before the pre-cue onset were extracted from the continuous MEG data. For the post-cue trials (attend left and right) epochs of 2.9 s after cue onset were derived from the MEG recordings for each participant. Movement artefacts and horizontal eye movements as monitored by the EOG were determined for each epoch by visual inspection and excluded from analysis. The number of trials analyzed for the pre-cue task and post-cue combinations (fixation left post-cue: M = 106.1 ± 2.0 s. e. m., fixation right post-cue: M = 106.8 ± 1.8 s. e. m., rings left post-cue: M = 104.9 ± 2.23 s. e. m., rings right-post-cue: M = 103.9 ± 2.16) were equal (main effect pre-cue task $F(1, 19) = 2.39$, $p = 0.138$, $\eta^2 = 0.11$; main effect post-cue $F(1, 19) = 0.02$, $p = 0.879$, $\eta^2 = 0.001$; interaction pre-cue task by post-cue: $F(1, 19) = 0.97$, $p = 0.336$, $\eta^2 = 0.05$). For each pre-cue task, post-cue condition and participant the epochs were averaged separately in order to obtain stimulus evoked MEG data epochs.

Cortical source estimation of ssVEF responses

Before the ssVEF responses were extracted from the averaged MEG data epochs, these evoked MEG responses were transformed into cortical source space by a weighted minimum norm estimation (wMNE) approach (Gramfort et al. 2014) using the brainstorm toolbox (*https://neuroimage.usc.edu/brainstorm/*). The source reconstruction of evoked MEG data epochs was based on a forward model based on an overlapping spheres head model (Huang et al. 1999) using a canonical cortical mesh (3003 vertices) derived from the ICBM152 template (Mazziotta et al. 2001). Thereby, the individual head and sensor positions of each

subject were co-registered with the template brain by realigning the individual with the template brain's fiducials and minimizing the mean distance between the individual head shape points and the template brain scalp surface (Moratti et al. 2011). Thereafter, the forward model was calculated by using a head model based on overlapping spheres (Huang et al. 1999). Finally, a weighted Minimum Norm Estimation (wMNE) (Gramfort et al. 2014) was used to calculate the current density of the evoked MEG averages (see above) on the cortical surface for later analysis. Finally, for illustration purposes and later statistical analysis, regions of interests (ROIs) were defined by overlaying a co-registered Brodmann Atlas as implemented in Brainstorm (Tadel et al., 2011;*https://neuroimage.usc.edu/brainstorm/*). The atlas contains V1, V2, and hMT+ areas and were extended by adding inferior-temporal visual cortex and the occipito-parietal brain area (see Figure 1 below).

In order to extract the ssVEF responses in cortical source space, the time series of the cortical current densities at each vertex of the cortical surface were demeaned and the 12 Hz and 15 Hz Fourier components were determined by a Fast Fourier Transform (FFT) using the fieldtrip toolbox (Oostenveld et al. 2011);*https://www.fieldtriptoolbox.org*). For the pre-cue baseline conditions (attend the central fixation cross vs. attend both peripheral rings), the 1 s epochs were zero padded to 10 s in order to obtain a frequency resolution of 0.1 Hz for the FFT. For the post-cue 2.9 s epochs overlapping four 1 s intervals were extracted (0.5 s to 1. 5 s, 1 s to 2 s, 1.5 s to 2.5 s and 2 s to 2.9 s). Each interval was zero padded to 10 s in order to obtain a 0.1 Hz frequency resolution and submitted to FFT analysis. Then, the obtained FFTs were averaged. Finally, for all FFTs (pre-cue baseline and post-cue intervals) the 12 Hz and 15 Hz power of the corresponding Fourier components were determined at each vertex of the canonical brain surface mesh.

Determination of cortical sources that significantly oscillated at the stimulus driven frequencies (12 Hz and 15 Hz)

We determined which cortical sources showed oscillatory neural activity at the driving ssVEF frequencies significantly different from background noise. As power estimates are the sum of two squared measures (real and imaginary parts), power estimates of the signal (here at the ssVEF frequency of interest) and noise (here at frequency bins different from the ssVEF frequencies of interest) follow a chi-square distribution (Dobie and Wilson 1996). Therefore, the power at the frequency of interest can be tested against noise by an F-ratio test with degrees of freedom $df = 2$ for the numerator and $df = 2m$ for the denominator, whereby m is the number of noise frequency bins (Dobie and Wilson 1996).

Using this method, we created two masks for the pre-cue central fixation cross task at 12 Hz and 15 Hz (flicker frequency for each visual hemifield was counter-balanced across subjects) based on the grand average power spectrum across all subjects, representing our signal. Noise was defined by 31 noise frequency bins between 17 Hz and 20 Hz (0.1 Hz steps), that were chosen as they did not contain any harmonics of the ssVEF responses. The sources included in the masks were parametrically determined by an F test with the corresponding degrees of freedom at a false discovery rate corrected alpha threshold of 0.05 (3003 comparisons, threshold at $F(2, 62) = 9.03$, $p_{\text{fdr corrected}} < 0.001$). Then, these two masks were OR logically combined into one mask for the pre-cue central fixation cross task. The same was done for the pre-cue peripheral rings task (threshold at $F(2, 62) = 10.12$, $p_{\text{fdr corrected}} < 0.001$). The two masks were created in order to compare the spatial extension of significant ssVEF responses in cortical source space between these two pre-cue baseline tasks (see Results).

Finally, a third mask was created by logically OR combining the source masks of the F-ratio tests on the grand means of power spectra of the fully balanced combinations of pre- and post-cue conditions (*e. g.* pre-cue baseline attend rings, post-cue lvf not attended, post-cue lvf attended, pre-cue baseline attend cross, post-cue lvf not attended, post-cue lvf attended, etc.). This was done in order not to bias the implicated sources in the mass-univariate statistical tests (see below) towards one pre- and post-cue task combination. The same parameters as described above were applied to these F-ratio tests (threshold at $F(2, 62) = 8.69$, $p_{\text{fdr corrected}} < 0.001$). Figure 1 depicts the resulting overall mask for the overall statistical comparisons (see below).

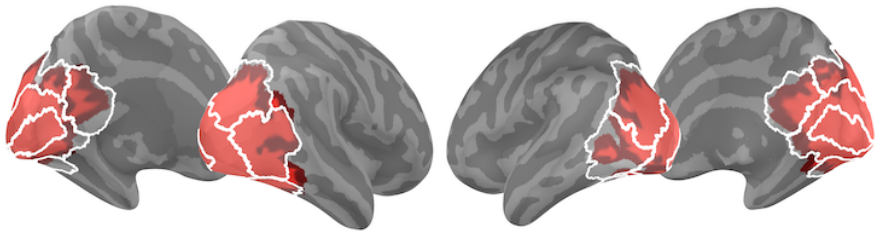

Figure 1: The right and left back view of the canonical brain surface and the Fourier components at 12 Hz and 15 Hz significantly different from noise are shown in red based on the combined F-ratio tests on the ssVEF signals of all condition combinations. The white lines indicate the boundaries between ROIs (V1, V2, hMT+, inferior-temporal and occipito-parietal cortex).

Statistical Analysis within the masked cortical source space

First, the oscillatory ssVEF responses between both pre-cue conditions (attend the central fixation cross vs. attend the peripheral rings) were compared using a non-parametric cluster-based permutation approach (Nichols and Holmes 2002) restricted to the cortical sources that oscillated at the stimulus driven frequencies significantly different from noise (see Figure 1). From these sources the relative power of the 12 Hz and 15 Hz driving frequencies were extracted by dividing the power values of interest by the mean power across the noise power bins (31 frequency bins between 17 Hz and 20 Hz in 0.1 Hz steps). Then, within the cortical source mask (Figure 1) source clusters were formed when at least one adjacent source neighbor indicated a significant difference based on a dependent t-test (cluster alpha threshold of $p = 0.025$ testing for both directions). Then, the t-values were summed across the cluster. Thereafter, 1000 random permutations between both pre-cue conditions for each cortical source under the Null hypothesis of no differences between attending the central fixation cross or the peripheral rings were done. At each permutation step the same cluster rule was applied and the maximum t cluster sum entered a permutation distribution. Finally, the empirically observed t clusters obtained by the first step (see above) with a sum exceeding the 97.5 percentile (test in both directions) of the permutation distribution were considered as significant. In order to test possible interactions of cortical hemisphere, mean relative ssVEF power were extracted from the resulting significant clusters (see Results) and compared with the mean ssVEF activity in the homologous opposite hemisphere by using a repeated measures ANOVA with within-subject factors pre-cue condition (fixation cross and peripheral rings) and hemisphere (left and right). Greenhouse-Geisser corrections were applied when necessary.

However, the main objective of this study was to characterize how stimulus driven ssVEF responses are modulated by shifts of spatial attention when spatial attention had been already directed towards the peripheral or central visual field (rings vs. cross). Using the same non-parametric cluster-based mass-univariate approach, the interaction of relative ssVEF power changes between experimental phases (pre-cue baseline, post-cue hemifield not attended or attended) and pre-cue baseline conditions (attend central fixation cross or peripheral rings) was assessed for the left and right visual hemifield stimulations, separately. However, clusters were derived from a dependent F-test (equivalent to a repeated measures ANOVA) comparing the differences in relative ssVEF power between the pre-cue peripheral rings minus central fixation condition, post-cue visual hemifield not attended when rings were attended before minus visual hemifield not attended when central fixation cross was attended before, and post-cue visual hemifield attended when rings were attended before minus visual hemifield attended when central fixation cross was attended before. Note, that the comparison of these differences is equivalent to test the interaction experimental phase by pre-cue condition. Source clusters were formed when at least one adjacent source neighbor indicated a significant interaction based on a dependent F-test (cluster alpha threshold of $p = 0.05$ testing for one direction). F-values were summed across the cluster. Then, the same permutation approach as outlined above was applied. However, the empirically observed F clusters with a sum exceeding the 95 percentile (F test in only one direction) of the permutation distribution were considered as significant. All non-parametric cluster-based permutation

tests were implemented using the fieldtrip toolbox (Oostenveld et al., 2011;*https://www.fieldtriptoolbox.org*).

In order to test any interactions with hemisphere, mean relative ssVEF power values of cortical source clusters of both hemispheres as obtained by the permutation statistics were entered in a repeated measures ANOVA with within-subject factors of pre-cue baseline, experimental phase and hemisphere. Greenhouse-Geisser corrections were applied when necessary.

ROI analysis

As the cluster-based permutation statistics indicated an interaction of pre-cue condition by experimental phase in source clusters covering various ROIs as defined by the co-registered brain atlas (see above), mean relative ssVEF power across sources that intersected with significant source clusters and ROI regions were analyzed with a repeated measures ANOVA with within-subject factors of pre-cue baseline, experimental phase and ROI collapsed across hemispheres for homologous left and right source clusters if both ROIs indicated an interaction in the previous cluster based permutation statistics. For ROIs that only indicated an interaction in the right hemisphere, only right hemisphere relative ssVEF power values were considered. Greenhouse-Geisser corrections were applied when necessary.

As this analysis revealed a significant pre-cue baseline by experimental phase by ROI interaction, a repeated measure ANOVA with within-subject factors of pre-cue baseline and experimental phase was fitted to the data for each ROI, separately. In order to detangle the observed interactions at each ROI, modulation differences between conditions were compared using paired t-tests (testing the difference of condition differences). Finally, mean relative ssVEF power within each ROI were contrasted between the two pre-cue baseline conditions (attend central fixation cross vs. attend both peripheral rings) using paired t-tests.

Results

Behavioral results

During the pre-cue baseline conditions participants detected on average 78.50 % (± 3.43 s. e. m.) of the luminance changes in both peripheral rings with a false alarm rate of 5.01 % (± 0.96 s. e. m.). Surprisingly, the performance during the central fixation cross task was worse with a mean detection rate of 57.58 % (± 4.28 s. e. m.) and a mean false alarm rate of 15.54 % (± 2.52 s. e. m.). However, in both pre-cue conditions performance was better than chance as for both tasks all individual d' indices were greater than zero (peripheral rings condition: range d' = 1.37 – 3.96; central fixation cross condition: range d' = 0.41 – 2.75). Therefore, all participants were engaged in the pre-cue tasks. In general, comparing the d' indices between the pre-cue conditions, participants were more sensitive detecting the luminance changes of the peripheral rings than the size changes of the central fixation cross ($t(19) = 7.01$, $p < 0.001$, Cohen's $d = 1.57$). However, participants applied the same response criteria for both tasks (mean c-index peripheral rings condition: 0.42 ± 0.09 s. e. m.; mean c-index central fixation cross task: 0.48 ± 0.10; $t(19) = -0.57$, $p = 0.575$, Cohen's $d = 0.13$).

During the post-cue task, participants detected on average 76.25 % (± 3.59 s. e. m.) of the luminance changes within a sector of the spatially cued ring with a false alarm rate of 1.66 % (± 0.49 s. e. m.). Mean d' indices of 3.32 (range: 1.44 to 4.79) indicated a high sensibility of the participants to detect the post-cue targets with an average response criteria c of 0.85 (± 0.11 s. e. m.).

Neuromagnetic oscillatory brain responses

First, we compared the oscillatory ssVEF responses in cortical source space between the two pre-cue conditions, in which subjects had to attend the central fixation cross or two peripheral flickering rings. Thereby, the dipoles on the canonical cortex surface that captured significant oscillatory ssVEF power different from background noise were determined by the F-ratio test (see Methods) for each pre-cue condition, separately. Figure 2 shows the power spectra and ssVEF topographies for both pre-cue conditions, and the spatial distribution of significantly oscillating cortical sources for the "attend to fixation cross" and "attend to both rings" conditions, respectively. Only cortical sources that exceeded the critical threshold of the F-ratio test

are shown (critical minimum F ratio: $F(2, 62) = 9.03$, $p_{\text{fdr corrected}} < 0.001$ for the central fixation condition; F ratio: $F(2, 62) = 10.12$, $p_{\text{fdr corrected}} < 0.001$ for the peripheral rings condition). Both pre-cue conditions resulted in ssVEF responses in V1, and V2 in both hemispheres, whereas attending to the peripheral flickers activated more extended ssVEF power modulations in right occipito-parietal, and hMT+ areas including a small part of the right pre-cuneus.

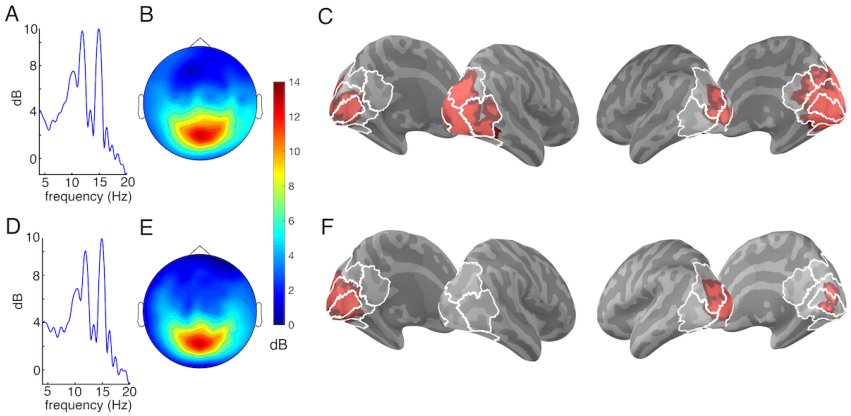

Figure 2: **(A)** The spectral decomposition, **(B)** the averaged 12 Hz and 15 Hz Fourier component topographies, and**(C)** the cortical sources for the 12 Hz and 15 Hz Fourier components significantly different from noise are shown (red clusters) for the attend to peripheral rings pre-cue condition. **(D, E, F)**The same information is shown for the attend to fixation cross pre-cue condition.

In addition to the descriptive reporting of the spatial distribution of significantly oscillating sources at the ssVEF driving frequencies of both pre-cue conditions, ssVEF responses to both pre-cue baselines were directly compared using cluster-based permutations statistics. A significant positive cluster indicated increased ssVEF power partly in right occipito-parietal, hMT+ and V2 areas when participants attended the peripheral rings instead of the central fixation cross (summed t-values = 82.23, p = 0.022, maximum parametric $t(19) = 3.39$, p = 0.003, Cohen's d = 0.76, see Figure 3A).

However, the absence of a left hemisphere effect does not automatically imply an interaction between the pre-cue condition (attend rings vs. attend cross) and hemisphere (left vs. right). Therefore, we extracted the ssVEF power values for the two pre-cue conditions in the homologous left hemisphere regions in order to test such an interaction by comparing the mean relative power across the corresponding cortical sources for each pre-cue condition in the left and right hemisphere. The observed interaction ($F(1, 19) = 7.78$, p = 0.012, $\eta^2 = 0.29$) corroborated the increased implication of the right occipito-parietal, hMT+ and V2 areas when both peripheral rings were attended (see Figure 3B).

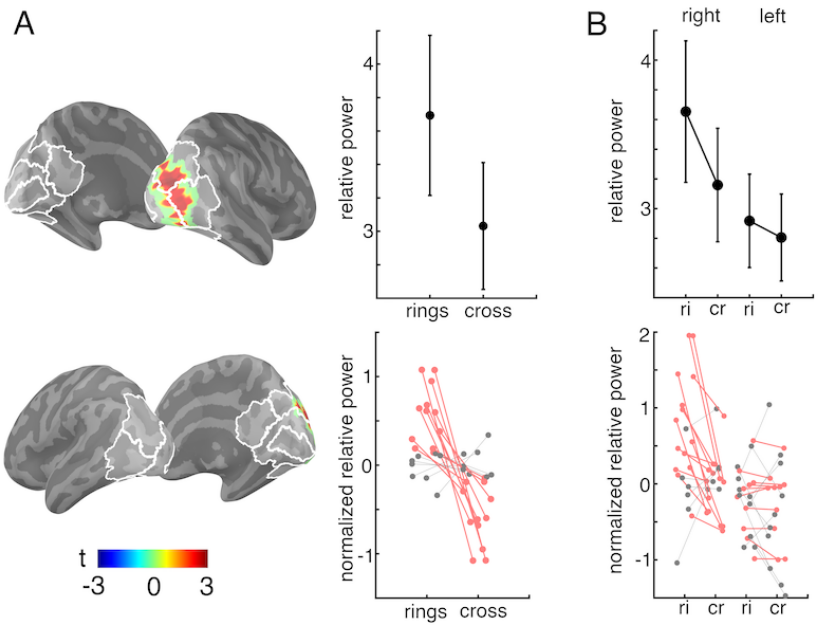

Figure 3: **(A)** The left column shows the significant cluster in cortical source space of the comparison between the "attend to both rings" and "attend to the central fixation cross" pre-cue conditions. The upper panel of the right columns depicts the mean relative power across the sources pertaining to the significant cluster. The lower panel shows the corresponding paired observation plot for mean normalized values. Red lines represent participants with a difference exceeding the lower bound of the 95% confidence interval of paired differences. Grey lines represent differences that did not meet this criterion. **(B)** The upper panel shows the mean power across the significant source cluster of (A) for the right and homologous left hemisphere regions. The lower panel depicts the corresponding paired observation plot for mean normalized values, so that individual differences can be observed at the same scale. Red lines for the right hemisphere represent participants with a difference exceeding the lower bound of the 95% confidence interval of differences. Grey lines represent data that do not meet this criterion. Red lines for the left hemisphere represent participants with a difference within the 95% confidence interval including zero (indicating the absence of an effect). Grey lines represent differences outside these boundaries. Error bars in all subplots indicate the s. e. m. ri = rings, cr = cross.

However, the main objective of this study was to characterize how stimulus driven ssVEF responses are modulated by shifts of spatial attention when spatial attention is already directed towards the peripheral or central visual field (rings vs. cross). Therefore, we assessed the interaction of relative ssVEF power changes across experimental phases (pre-cue baseline, left or right visual hemifield not attended or attended) and pre-cue baseline condition (rings vs. cross). The nonparametric cluster-based permutation test based on previously formed F clusters (see methods) for the left visual hemifield (lvf) stimulation indicated an interaction between the pre-cue baseline condition (attend rings vs. central fixation cross) and experimental phase (pre-cue baseline, lvf not attended, lvf attended). The significant source cluster encompassed V1, V2, hMT+, the occipito-parietal and inferior-temporal visual cortex of the right hemisphere (summed F value = 1044, $p < 0.001$, maximum parametric $F(2, 38) = 9.71$, $p < 0.001$, $\varepsilon = 0.84$, $\eta^2 = 0.34$; Figure 4A). However, right visual hemifield stimulation (rvf) resulted in an interaction between pre-cue baseline condition and experimental phase only at trend level localized in left V1, V2, and a small part of the occipital-parietal region (summed F = 137, $p = 0.084$; maximum parametric $F(2, 38) = 8.09$, $p = 0.004$, $\varepsilon = 0.73$, $\eta^2 = 0.30$, Figure 4A).

Given the height of the left hemispheric cluster ($F(2, 38) = 8.09$) the trend level cluster based significance

was probably due to the smaller extension of the source cluster. Therefore, in order not to rule out a significant interaction for the rvf stimulation in the left hemisphere, the mean ssVEF power values across the significant source clusters of the left and right hemispheres were entered in a repeated measurements ANOVA with the within-subject factors pre-cue baseline, experimental phase and hemisphere. An absent interaction between the pre-cue baseline condition and experimental phase in the left hemisphere should result in a pre-cue baseline by experimental phase by hemisphere interaction. However, no such interaction was observed ($F(2, 38) = 1.66$, $p = 0.20$, $\varepsilon = 0.93$, $\eta^2 = 0.08$). Across hemispheres, the interaction pre-cue baseline by experimental phase indicated that ssVEF power was differently modulated depending on the pre-cue baseline condition ($F(2, 38) = 8.57$, $p < 0.001$, $\varepsilon = 0.71$, $\eta^2 = 0.31$). Figure 4B depicts the mean relative ssVEF power changes across all significant cortical sources pertaining to the previously identified source clusters in the left and right cortical hemisphere for all experimental phases (pre-cue baseline, post-cue not attended, and post-cue attended) and the two different pre-cue baseline conditions (attend rings vs. fixation cross). Whereas the participants attended the peripheral rings during the pre-cue baseline task, the ssVEF responses across both cortical source clusters were enhanced for the pre-cue baseline and post-cue attend experimental phases compared to the unattended visual hemifield (pre-cue vs. unattended: $t(19) = 3.80$, $p = 0.001$, Cohen's $d = 0.85$; attended vs. unattended: $t(19) = 4.24$, $p < 0.001$, Cohen's $d = 0.95$). However, when the participants attended to small variations of fixation cross sizes during the pre-cue experimental phase, relative ssVEF power was similar to the ssVEF response elicited by the unattended hemifield stimulation during the post-cue phase ($t(19) = 1.68$, $p = 0.110$, Cohen's $d = 0.37$). In contrast, attending the cued hemifield during the post-cue phase provoked enhanced ssVEF responses in comparison when the hemifield was not attended ($t(19) = 4.43$, $p < 0.001$, Cohen's $d = 0.99$). Furthermore, when we tested the activation level for the attended side between the conditions cross vs. rings we found a trend for higher activation when subjects attended to central fixation first ($t(19) = 1.93$, $p = 0.070$, Cohen's $d = 0.43$).

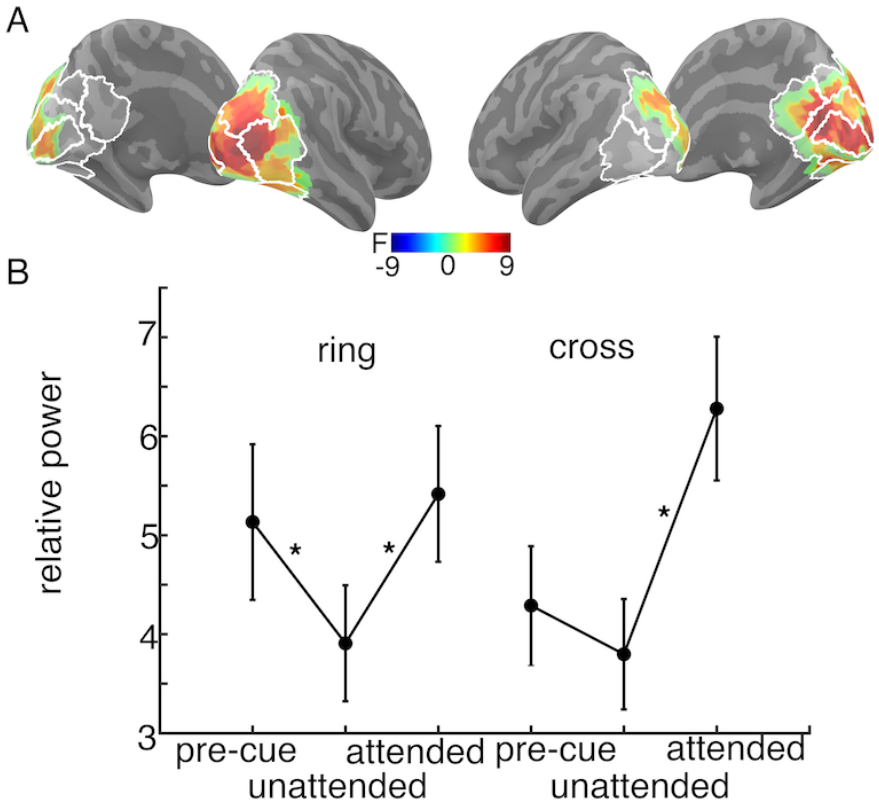

Figure 4: (A) Both, the significant right hemispheric and trend level left hemispheric, source clusters are shown. The color bar indicates F-values. **(B)** The mean relative ssVEF power changes across source clusters in (A) are shown for the pre-cue baseline, post-cue unattended, and post-cue attended experimental phases separated by the pre-cue ring and fixationcross conditions. The error bars depict s. e. ms. * $p < 0.05$

As the observed effects were spread across different cortical regions within the visual cortex, mean ssVEF relative power changes for each region of interest (ROIs) were entered in a repeated measure ANOVA with within-subject factors pre-cue condition (rings vs. cross), experimental phase (pre-cue baseline, not attend and attend cued visual hemifield), and ROIs (V1, V2, precuneus, occipito-parietal cortex, hMT+, and inferior-temporal cortex). Relative power values for homologous left and right cortical areas that both covered significant clusters from the previous analysis were collapsed across hemispheres, whereas for the remaining ROIs only right hemisphere ssVEF responses entered the analysis.

A significant pre-cue condition by experimental phase by ROIs interaction, indicated that the previously reported pre-cue condition by experimental phase interaction is different depending on the ROI ($F(10, 190) = 4.03$, $p = 0.008$, $\varepsilon = 0.11$, $\eta^2 = 0.17$). Therefore, the pre-cue condition by experimental phase interaction was assessed separately for ROI (see Figure 5A). At each ROI a significant pre-cue condition by experimental phase interaction was observed (Table 1).

ROI	$F(2, 38)$	p	ε	η^2
V1	6.48	0.010	0.41	0.25
V2	6.78	0.009	0.39	0.26
precun	6.32	0.006	0.61	0.25
occip-par	8.69	0.003	0.48	0.31
hMT+	6.39	0.009	0.54	0.25
inf-temp	5.16	0.014	0.50	0.21

Table 1: Results of the repeated measures ANOVA pre-cue condition by experimental phase are shown for each ROI. precun = precuneus, occip-par = occipito-parietal, inf-temp = inferior-temporal, hMT+ = human middle temporal.

The left column of Figure 5B shows the mean relative power ssVEF modulations for the pre-cue baseline, post-cue not attended and attended conditions separated by the pre-cue condition (attend peripheral rings vs. attend central fixation cross). The interaction pre-cue condition by experimental phase in V1, V2, precuneus, and occipito-parietal cortex was explained by bigger ssVEF modulations by spatial attention to the cued visual hemifield when the central fixation cross was attended during the pre-cue baseline compared to when the peripheral rings had been attended (t-tests between the modulation differences V1: $t(19) = 2.69$, $p = 0.014$, Cohen's $d = 0.60$; V2: $t(19) = 2.53$, $p = 0.020$, Cohen's $d = 0.57$; precuneus: $t(19) = 2.59$, $p = 0.018$, Cohen's $d = 0.58$; occipito-parietal cortex: $t(19) = 2.39$, $p = 0.027$, Cohen's $d = 0.54$; see Figure 5B).

However, this was not the case for the hMT+ and inferior-temporal cortical areas (hMT+: $t(19) = 1.33$, $p = 0.20$, Cohen's $d = 0.30$; inferior-temporal cortex: $t(19) = 0.77$, $p = 0.45$, Cohen's $d = 0.17$). Critically, when the participants attended the central fixation cross during the pre-cue baseline, the peripheral ring flickers did not evoke greater ssVEF responses than when spatial attention was directed away to the cued visual hemifield (not attended post-cue condition) in these brain regions. However, this modulation difference was greater when participants attended the peripheral rings during the pre-cue baseline (t-tests between the modulation differences hMT+: $t(19) = 3.10$, $p = 0.006$, Cohens' $d = 0.69$; inferior-temporal cortex: $t(19) = 2.83$, $p = 0.011$, Cohen's $d = 0.63$; see Figure 5B).

Finally, given the ssVEF modulation patterns in each ROI (see Figure 5), the two pre-cue baseline conditions (rings vs. cross) were compared directly for each ROI, separately. In V1, V2, and precuneus no differences

were observed (ps > 0.05), whereas in the occipito-parietal area attending to both peripheral rings elicited greater ssVEF responses than when attending to the fixation cross changes ($t(19) = 2.15$, $p = 0.045$, Cohen's $d = 0.48$). This effect was pronounced in hMT+ ($t(19) = 3.13$, $p = 0.006$, Cohen's $d = 0.70$) and inferio-temporal cortex ($t(19) = 2.39$, $p = 0.027$, Cohen's $d = 0.53$).

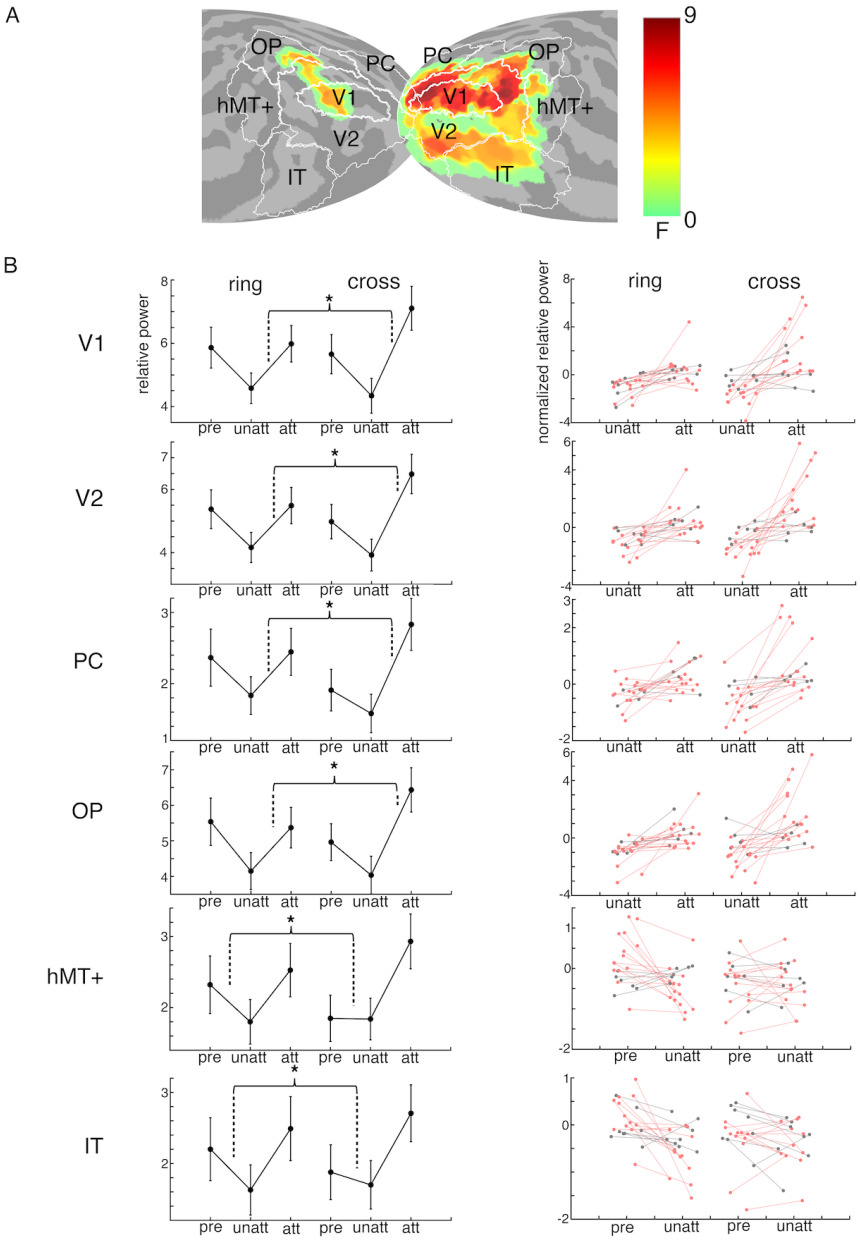

Figure 5: **(A)** The left panel shows the cluster in cortical source space for the interaction experimental phase (pre-cue baseline, post-cue not attended and attended) by pre-cue baseline condition (rings vs. cross) in the right hemisphere for the lvf flickers. The trend level cluster for this interaction is also shown in the left hemisphere for the rvf flickers. The source map was projected onto a plane with the ROI labels using the Mollweide method. **(B)** The left row shows the mean relative ssVEF power changes across the dipoles within each ROI for the experimental phase by pre-cue baseline condition for each ROI. The black brackets with

the dashed lines indicate the significant differences of modulation differences between conditions (see main text for the t-tests between differences * $p < 0.05$). The right row depicts the corresponding single paired observations plots. The red lines indicate participants with ssVEF modulation differences greater that the lower bound of the corresponding 95% CI interval not containing zero. The grey lines represent participants that do not fulfill that criterion. Note, that for better visibility the relative ssVEF power values were mean normalized. Error bars in all subplots represent the s. e. m. RFV = right visual hemifield stimulation, LVF = left visual hemifield stimulation. PC = precuneus, OP = occipito-parietal, IT = inferior temporal, hMT+ = human middle temporal area.

Discussion

The aim of the present MEG study was to identify areas in the visual cortex of the human brain that contribute to an attentional enhancement of steady state amplitudes with attention. In a typical spatial attention task, after a baseline period, subjects were given an instructive cue to shift attention to the left or right visual hemifield and to perform a task at the to-be-attended side. Different from many studies, we controlled for the attentional deployment before the cue by instructing to either attend to central fixation or to both stimuli in the left and right visual hemifield, respectively. Compliance was assured by having a task at the respective location during the baseline as well as in the post-cue period. With this manipulation, we were able to test SSVEF sensory gain modulations for peripheral stimuli under the conditions that attentional resources were shifted to this peripheral stimulus (attend cross) or away from an already attended peripheral stimulus (attend rings). Behavioral data showed that subjects were compliant with the task, although the "attend cross" condition seemed to be more difficult compared to the "attend rings" baseline condition.

Comparing the baseline conditions, we found a differential activation in early visual cortex. In particular, when subjects were instructed to attend to both rings, activation was not just restricted to V1 and V2, as for the "attend cross" baseline, but also included occipito-parietal cortex, and hMT+. Given that hMT+ was only activated in the "attend rings" pre-cue baseline period is in line with previous reports on hMT+ activation by motion and also by flickering stimuli (Treue and Martinez-Trujillo 1999, Huk and Heeger 2002, Palomares et al. 2012). Surprising to us was that this additional activation in that baseline condition was more prominent in the right cortical hemisphere (but numerically in the left hemisphere as well, see Figure 3B), whereas V1/V2 activation was clearly located in both hemispheres.

The attentional activation pattern after the cue, relative to pre-cue baseline across all areas, was different for the two pre-cue conditions. When subjects first attended to both rings in the left and right visual hemifield, cortical activation slightly increased for the side for which attention was maintained, but significantly decreased for the side for which attention was withdrawn. If, however, participants first attended to central fixation, cortical activation was significantly increased for the to-be-attended stimulus, and data revealed a trend for this activation boost to be even bigger compared to when subjects attended to both rings first. For the to-be-ignored side, activation remained basically on the pre-cue baseline level.

However, a closer inspection on the individual activation pattern of the respective cortical areas resembled an interactive activation pattern that not only depended on the pre-cue condition but also on the visual area. When subjects attended to both rings first, we observed a reduction in activity in areas V1, V2, pre-cuneus, occipital parietal and inferior-temporal cortex for the to-be-ignored stimulus, whereas for the to-be-attended ring activity basically remained at the pre-cue level. Thus, all areas followed the pattern we observed in the test across all areas (see above). Critically, when subjects attended to the fixation cross first, the SSVEF modulation patterns differed significantly between the cortical areas within the visual cortex. In V1, V2, pre-cuneus and occipital parietal cortex SSVEF power followed a similar pattern as during the pre-cue attend to both rings baseline. The SSVEF amplitudes elicited by the to-be-ignored hemifield flickers were suppressed. However, the to-be-attended flickers generated a greater SSVEF power boost after participants attended the central fixation cross than after having split their attention between both hemifields during the ring pre-cue baseline task. On the contrary, hMT+ and inferior-temporal cortex did not show a further reduction in activity for the to-be-ignored ring and no enhanced boost of SSVEF amplitudes for the to-be-attended hemifield after the fixate central cross pre-cue task.

The present observations nicely match our very simple previous source reconstructions of EEG data in feature-based attention (Andersen et al. 2008, Andersen and Müller 2010). When subjects attended to red or blue spatially superimposed random dot kinematograms (RDKs) we also found the sources of the attention effect in early visual cortex only, including V1/V2. While it is quite clear that V1/V2 show prominent responses to flicker stimuli in the respective stimulation frequency plus its harmonics (Rager and Singer 1998) it is still unknown how far flicker responses propagate in the visual processing hierarchy. A number of physiological restrictions suggest that propagation is restricted to areas of early visual cortex, due to dendritic low-pass filtering, in particular for higher flicker frequencies (Fortune and Rose 1997, Vaidya and Johnston 2013), increase in receptive field size (Hubel and Wiesel 1968), or synaptic input from cells that respond to different flicker frequencies, resulting in so-called intermodulation frequencies (Zemon and Ratcliff 1984). The idea that propagation of the respective driving frequencies is limited to early processing stages was also demonstrated in fMRI (Di Russo et al. 2007, Palomares et al. 2012).

The activation pattern in early visual cortex when subjects first attended central fixation nicely resembles the pattern of SSVEP amplitude time courses in spatial shifting designs (Müller et al. 1998, Müller 2008). In these studies, SSVEP amplitude for the to-be-ignored side remained on pre-cue baseline level, whereas SSVEP amplitude for the to-be-attended side exhibited a significant increase. However, the pattern of amplitude modulations differed in study by Gundlach and colleagues (2020) that used the same design as in the present study. In this study, when subjects first attended to the fixation cross, an increase in SSVEP amplitudes for both, the to-be-attended and unattended side was found, of course with a significantly greater increase for the to-be-attended side. When subjects attended to both rings first, we found no change in amplitude for the side that needed to be ignored after the cue, but only a significant increase for the then selected side. The difference between the more recent and the previous studies may lie in the fact that in the most recent study we used a very broad range of posterior electrodes including midline electrodes, whereas in the two older studies we only used one posterior-temporal electrode left/right, respectively for SSVEP time course analysis. This broader cluster might have picked-up activity from many more cortical areas. In previous studies we have shown that the pattern of SSVEP amplitude modulation is not identical over a broader range of electrodes as used in the 2020 study (Andersen et al. 2012, Müller et al. 2018), and therefore, it might be of interest to reanalyze this data with a more temporal and much smaller electrode cluster, or even single electrodes. In addition, as the focus of the work by Gundlach and colleagues (2020) focused on the relationship between SSVEP and alpha-band modulations in a spatial cueing paradigm, the SSVEP amplitudes were derived from single-trial FFT spectra. With such an analysis, induced activity of non-phase locked ongoing neural oscillatory activity is not averaged out and may contribute to the SSVEP amplitude estimates in the same frequency range. In the current study, however, SSVEP amplitude values were derived from trial-averaged FFT spectra promoting evoked signals such as SSVEPs while minimizing induced signals such as endogenous neural activity not phase locked to the stimulation. While the relative amplitude patterns (attended > unattended) are comparable, differences in the absolute amplitude may stem from differences in foundations of the signals revealed by different analysis approaches.

To summarize: The present study replicated previous studies that located cortical sources of SSVEPs driven by flickering (frequency-tagged) stimuli in early visual cortex. Our results complement and extend these studies showing that early visual cortex also drives attentional modulations of SSVEP amplitudes. While the activation pattern in V1/V2 was consistent, the specific modulatory effects differed across different regions within early visual cortex with a distinct pattern further up in the processing hierarchy in areas such as hMT+ and inferior-temporal cortex in the present case. Nevertheless, results again demonstrate the power of frequency-tagged stimuli to investigate attentional competitive interactions in multi-element stimulus displays. To what extent a certain area that is specialized in processing of a certain feature, such as V4 for color, contributes significantly more to the observed SSVEP amplitude modulations in color processing, compared to the other areas that "just" follow the on/off is subject to a current project and we will report the results in the nearer future.

References

Adamian, N., S. K. Andersen and S. A. Hillyard (2020). "Parallel attentional facilitation of features and objects in early visual cortex." *Psychophysiology* **57** (3).

Adler, J., C. M. Giabbiconi and M. M. Müller (2009). "Shift of attention to the body location of distracters is mediated by perceptual load in sustained somatosensory attention." *Biological Psychology***81** : 77-85.

Andersen, S. K., S. A. Hillyard and M. M. Müller (2008). "Attention facilitates multiple stimulus features in parallel in human visual cortex." *Curr Biol* **18** (13): 1006-1009.

Andersen, S. K., S. A. Hillyard and M. M. Müller (2013). "Global facilitation of attended features is obligatory and restricts divided attention." *Journal of Neuroscience* **33** (46): 18200-18207.

Andersen, S. K. and M. M. Müller (2010). "Behavioral performance follows time-course of neural facilitation and suppression during cued shifts of feature-selective attention." *PNAS* **107** : 13878-13882.

Andersen, S. K., M. M. Müller and S. A. Hillyard (2015). "Attentional selection of feature conjunctions is accomplished by parallel and independent selection of single features." *J Neurosci***35** (27): 9912-9919.

Andersen, S. K., M. M. Müller and J. Martinovic (2012). "Bottom-Up Biases in Feature-Selective Attention." *Journal of Neuroscience***32** (47): 16953-16958.

Antonov, P. A., R. Chakravarthi and S. K. Andersen (2020). "Too little, too late, and in the wrong place: Alpha band activity does not reflect an active mechanism of selective attention." *Neuroimage***219** : 117006.

Brummerloh, B., C. Gundlach and M. M. Muller (2019). "Attentional Facilitation of Constituent Features of an Object Does Not Spread Automatically along Object-defining Cortical Boundaries." *J Cogn Neurosci* **31** (2): 278-287.

Brummerloh, B. and M. M. Müller (2019). "Time matters: Feature-specific prioritization follows feature integration in visual object processing."*Neuroimage* **196** : 81-93.

Di Russo, F., S. Pitzalis, T. Aprile, G. Spitoni, F. Patria, A. Stella, D. Spinelli and S. A. Hillyard (2007). "Spatiotemporal analysis of the cortical sources of the steady-state visual evoked potential."*Human Brain Mapping* **28** : 323-334.

Dobie, R. A. and M. J. Wilson (1996). "A comparison of t test, F test, and coherence methods of detecting steady-state auditory-evoked potentials, distortion-product otoacoustic emissions, or other sinusoids." *J Acoust Soc Am* **100** (4 Pt 1): 2236-2246.

Fawcett, I. P., G. R. Barnes, A. Hillebrand and K. D. Singh (2004). "The temporal frequency tuning of human visual cortex investigated using synthetic aperture magnetometry." *NeuroImage* **21** : 1542-1553.

Fortune, E. S. and G. J. Rose (1997). "Passive and active membrane properties contribute to the temporal filtering properties of midbrain neurons in vivo." *Journal of Neuroscience* **17** (10): 3815-3825.

Giabbiconi, C. M., N. J. Trujillo-Barreto, T. Gruber and M. M. Müller (2007). "Sustained spatial attention to vibration is mediated in primary somatosensory cortex." *NeuroImage* **35** : 255-262.

Goltz, D., C. Gundlach, T. Nierhaus, A. Villringer, M. Muller and B. Pleger (2015). "Connections between Intraparietal Sulcus and a Sensorimotor Network Underpin Sustained Tactile Attention."*Journal of Neuroscience* **35** (20): 7938-7949.

Gramfort, A., M. Luessi, E. Larson, D. A. Engemann, D. Strohmeier, C. Brodbeck, L. Parkkonen and M. S. Hamalainen (2014). "MNE software for processing MEG and EEG data." *Neuroimage* **86** : 446-460.

Gundlach, C., N. Forschack and M. M. Müller (2022). "Suppression of Unattended Features Is Independent of Task Relevance." *Cerebral Cortex* **32** (11): 2437-2446.

Gundlach, C., S. Moratti, N. Forschack and M. M. Muller (2020). "Spatial Attentional Selection Modulates Early Visual Stimulus Processing Independently of Visual Alpha Modulations." *Cereb Cortex***30** (6): 3686-3703.

Hillyard, S. A., H. Hinrichs, C. Tempelmann, S. T. Morgan, J. C. Hansen, H. Scheich and H. J. Heinze (1997). "Combining steady-state visual evoked potentials and fMRI to localize brain activity during selective attention." *Human Brain Mapping* **5** : 287-292.

Huang, M. X., J. C. Mosher and R. M. Leahy (1999). "A sensor-weighted overlapping-sphere head model and exhaustive head model comparison for MEG." *Phys Med Biol* **44** (2): 423-440.

Hubel, D. H. and T. N. Wiesel (1968). "Receptive Fields and Functional Architecture of Monkey Striate Cortex." *Journal of Physiology-London* **195** (1): 215-243.

Huk, A. C. and D. J. Heeger (2002). "Pattern-motion responses in human visual cortex." *Nature Neuroscience* **5** (1): 72-75.

Kaufmann, C., G. K. Elbel, C. Gossl, B. Putz and D. P. Auer (2001). "Frequency dependence and gender effects in visual cortical regions involved in temporal frequency dependent pattern processing." *Human Brain Mapping* **14** (1): 28-38.

Kleiner, M., D. Brainard, D. Pelli, A. Ingling, R. Murray and C. Broussard (2007). "What's new in psychtoolbox-3." *Perception***36** : 1.

Linden, R. D., T. W. Picton, G. Hamel and K. P. Campbell (1987). "Human auditory steady-state evoked potentials during selective attention." *Electroencephalogr Clin Neurophysiol* **66** .

Makeig, S., M. M. Müller and B. Rockstroh (1996). "Effects of voluntary movements on early auditory brain responses." *Exp. Brain Res.***110** : 487-492.

Mazziotta, J., A. Toga, A. Evans, P. Fox, J. Lancaster, K. Zilles, R. Woods, T. Paus, G. Simpson, B. Pike, C. Holmes, L. Collins, P. Thompson, D. MacDonald, M. Iacoboni, T. Schormann, K. Amunts, N. Palomero-Gallagher, S. Geyer, L. Parsons, K. Narr, N. Kabani, G. Le Goualher, D. Boomsma, T. Cannon, R. Kawashima and B. Mazoyer (2001). "A probabilistic atlas and reference system for the human brain: International Consortium for Brain Mapping (ICBM)." *Philos Trans R Soc Lond B Biol Sci* **356** (1412): 1293-1322.

Moratti, S., C. Saugar and B. A. Strange (2011). "Prefrontal-occipitoparietal coupling underlies late latency human neuronal responses to emotion." *J Neurosci* **31** (47): 17278-17286.

Morgan, S. T., J. C. Hansen and S. A. Hillyard (1996). "Selective attention to stimulus location modulates the steady state visual evoked potential." *PNAS* **93** : 4770-4774.

Müller, M. M. (2008). "Location and features of instructive spatial cues do not influence the time course of covert shifts of visual spatial attention." *Biological Psychology* **77** : 292-303.

Müller, M. M. (2014). Neural mechanisms of feature-based attention. *Cognitive electrophysiology of attention* . G. R. Mangun. Amsterdam, Elsevier**:** 123-135.

Müller, M. M., S. Andersen, H. J. Trujilllo, P. Valdes Sosa, P. Malinowski and S. A. Hillyard (2006). "Feature-selective attention enhances color signals in early visual areas of the human brain." *PNAS* **103** : 14250-14254.

Müller, M. M., C. Gundlach, N. Forschack and B. Brummerloh (2018). "It takes two to tango: Suppression of task-irrelevant features requires (spatial) competition." *Neuroimage* **178** : 485-492.

Müller, M. M. and R. Hübner (2002). "Can the attentional spotlight be shaped like a doughnut? Evidence from steady state visual evoked potentials." *Psychological Science* **13** : 119-124.

Müller, M. M., P. Malinowski, T. Gruber and S. A. Hillyard (2003). "Sustained division of the attentional spotlight." *Nature***424** : 309-312.

Müller, M. M., T. W. Picton, P. Valdes-Sosa, P. Riera, W. Teder-Sälejärvi and S. A. Hillyard (1998). "Effects of spatial selective attention on the steady-state visual evoked potential in the 20-28 Hz range." *Cognitive Brain Research* **6** : 249-261.

Müller, M. M., W. Teder and S. A. Hillyard (1997). "Magentoencephalographic recording of steady-state visual evoked cortical activity." *Brain Topography* **9** : 163-168.

Müller, M. M., W. Teder-Sälejärvi and S. A. Hillyard (1998). "The time course of cortical facilitation during cued shifts of spatial attention." *Nature Neuroscience* **1** : 631-634.

Nichols, T. E. and A. P. Holmes (2002). "Nonparametric permutation tests for functional neuroimaging: a primer with examples." *Hum Brain Mapp* **15** (1): 1-25.

Norcia, A. M., L. G. Appelbaum, J. M. Ales, B. R. Cottereau and B. Rossion (2015). "The steady-state visual evoked potential in vision research: A review." *J Vis* **15** (6): 4.

Oostenveld, R., P. Fries, E. Maris and J. M. Schoffelen (2011). "FieldTrip: Open source software for advanced analysis of MEG, EEG, and invasive electrophysiological data." *Comput Intell Neurosci***2011** : 156869.

Palomares, M., J. M. Ales, A. R. Wade, B. R. Cottereau and A. M. Norcia (2012). "Distinct effects of attention on the neural responses to form and motion processing: A SSVEP source-imaging study." *Journal of Vision* **12** (10).

Pang, C. and M. M. Müller (2015). "Competitive interactions in somatosensory cortex for concurrent vibrotactile stimulation between and within hands." *Biological Psychology* **110** : 91-99.

Pastor, M. A., J. Artieda, J. Arbizu, M. Valencia and J. C. Masdeu (2003). "Human cerebral activation during steady-state visual-evoked responses." *The Journal of Neuroscience* **23** : 11621-11627.

Pastor, M. A., M. Valencia, J. Artieda, M. Alegre and J. C. Masdeu (2007). "Topography of cortical activation differs for fundamental and harmonic frequencies of the steady-state visual-evoked responses. An EEG and PET $H_2{}^{15}O$ Study." *Cerebral Cortex* **17** : 1899-1905.

Picton, T. W., M. S. John, A. Dimitrijevic and D. Purcell (2003). "Human auditory steady-state response." *International Journal of Audiology* **42** : 177-219.

Rager, G. and W. Singer (1998). "The response of cat visual cortex to flicker stimuli of variable frequency." *European Journal of Neuroscience* **10** : 1856-1877.

Snyder, A. Z. (1992). "Steady-state vibration evoked potentials: description of technique and characterization of responses." *Electroenceph. clin. Neurophysiol.* **84** : 257-268.

Störmer, V. S. and G. A. Alvarez (2014). "Feature-Based Attention Elicits Surround Suppression in Feature Space." *Current Biology***24** (17): 1985-1988.

Tadel, F., S. Baillet, J. C. Mosher, D. Pantazis and R. M. Leahy (2011). "Brainstorm: a user-friendly application for MEG/EEG analysis." *Comput Intell Neurosci* **2011** : 879716.

Taulu, S. and R. Hari (2009). "Removal of magnetoencephalographic artifacts with temporal signal-space separation: demonstration with single-trial auditory-evoked responses." *Hum Brain Mapp***30** (5): 1524-1534.

Tobimatsu, S., Y. M. Zhang and M. Kato (1999). "Steady-state vibration somatosensory evoked potentials: physiological characteristics and tuning function." *Clinical Neurophysiology* **110** : 1953-1958.

Treue, S. and C. M. Martinez-Trujillo (1999). "Feature-based attention influences motion processing gain in macaque visual cortex." *Nature* **399** : 575-579.

Vaidya, S. P. and D. Johnston (2013). "Temporal synchrony and gamma-to-theta power conversion in the dendrites of CA1 pyramidal neurons." *Nature Neuroscience* **16** (12): 1812-1820.

Walter, S., C. Quigley and M. M. Mueller (2014). "Competitive Interactions of Attentional Resources in Early Visual Cortex during Sustained Visuospatial Attention within or between Visual Hemifields: Evidence for the Different-hemifield Advantage." *Journal of Cognitive Neuroscience* **26** (5): 938-954.

Wieser, M. J. and A. Keil (2011). "Temporal Trade-Off Effects in Sustained Attention: Dynamics in Visual Cortex Predict the Target Detection Performance during Distraction." *Journal of Neuroscience* **31** (21): 7784-7790.

Woldorff, M. G. and S. A. Hillyard (1991). "Modulation of early auditory processing during selective listening to rapidly presented tones." *Electroenceph. clin. Neurophysiol.* **79** : 170-191.

Zemon, V. and F. Ratcliff (1984). "Intermodulation components of the visual evoked potential: Responses to lateral and superimposed stimuli." *Biological Cybernetics* **50** : 401-408.

Zhu, D., J. Bieger, G. Garcia Molina and R. M. Aarts (2010). "A survey of stimulation methods used in SSVEP-based BCIs." *Comput Intell Neurosci* **2010** : 702357.

Hosted file

`Table_1_Moratti_12_06_2023.docx` available at https://authorea.com/users/628230/articles/648890-distinct-patterns-of-spatial-attentional-modulation-of-steady-state-visual-evoked-magnetic-fields-ssvefs-in-subdivisions-of-the-human-early-visual-cortex